Nucleotide excision repair by dual incisions in plants

Fazile Canturk[a,b,1], Muhammet Karaman[a,c,1], Christopher P. Selby[a,1], Michael G. Kemp[a], Gulnihal Kulaksiz-Erkmen[a,d], Jinchuan Hu[a], Wentao Li[a], Laura A. Lindsey-Boltz[a], and Aziz Sancar[a,2]

[a]Department of Biochemistry and Biophysics, University of North Carolina School of Medicine, Chapel Hill, NC 27599; [b]Department of Biophysics, University of Erciyes School of Medicine, 38039 Kayseri, Turkey; [c]Department of Chemistry, Faculty of Arts and Sciences, Kilis 7 Aralık University, 79000 Kilis, Turkey; and [d]Department of Biochemistry, Hacettepe University Faculty of Medicine, Sıhhiye, 06100 Ankara, Turkey

Contributed by Aziz Sancar, March 16, 2016 (sent for review March 2, 2016; reviewed by Shisheng Li, Chentao Lin, and Yong-Jie Xu)

Plants use light for photosynthesis and for various signaling purposes. The UV wavelengths in sunlight also introduce DNA damage in the form of cyclobutane pyrimidine dimers (CPDs) and pyrimidine (6-4) pyrimidone photoproducts [(6-4)PPs] that must be repaired for the survival of the plant. Genome sequencing has revealed the presence of genes for both CPD and (6-4)PP photolyases, as well as genes for nucleotide excision repair in plants, such as *Arabidopsis* and rice. Plant photolyases have been purified, characterized, and have been shown to play an important role in plant survival. In contrast, even though nucleotide excision repair gene homologs have been found in plants, the mechanism of nucleotide excision repair has not been investigated. Here we used the in vivo excision repair assay developed in our laboratory to demonstrate that *Arabidopsis* removes CPDs and (6-4)PPs by a dual-incision mechanism that is essentially identical to the mechanism of dual incisions in humans and other eukaryotes, in which oligonucleotides with a mean length of 26–27 nucleotides are removed by incising ∼20 phosphodiester bonds 5′ and 5 phosphodiester bonds 3′ to the photoproduct.

DNA repair | UV light | DNA damage | plants | excision nuclease

Plants and other organisms that depend on photosynthesis are, by necessity, exposed to more sunlight than other organisms that are chemotrophs or heterotrophs. Hence, plants are expected to receive more exposure to UV wavelengths of light than other organisms. The genotoxic effects of UV are somewhat mitigated by the reflection of UV by the waxy leaf surface and absorbance of UV by the intracellular pigments that are present at high concentration in plant cells, including carotenoids and flavonoids. Nevertheless, plants still receive considerable amounts of DNA-damaging UV radiation and therefore must have the means to cope with the damage to ensure their survival. Indeed, DNA sequencing has revealed that plant genomes contain genes that are homologous to the genes of all major DNA repair pathways, including photoreactivation, nucleotide excision repair, base excision repair, and recombination/double-strand break repair (1–6).

However, biochemical studies of these DNA repair mechanisms have been limited. Of significance, *Arabidopsis* photolyases have been expressed in heterologous systems, purified, and characterized (7–9). Similarly, some of the enzymes of the base excision repair and recombination/double-strand break repair systems have been studied. In contrast, there have been no mechanistic studies on plant nucleotide excision repair, although it is known that plants can remove cyclobutane pyrimidine dimers (CPDs) and pyrimidine (6-4) pyrimidone photoproducts [(6-4)PPs] in a photolyase-independent manner (6, 10, 11), presumably by nucleotide excision repair. Here, we have used an *Arabidopsis* cell line and the in vivo excision assay recently developed in our laboratory (12–14) to demonstrate that *Arabidopsis* removes these photoproducts by dual incisions in a manner that is virtually identical to human nucleotide excision repair.

Results

Nucleotide Excision Repair. Although repair of UV photoproducts by light-dependent and -independent mechanisms in plants has been reported previously, there has not been a direct comparison of the two modes of repair under similar conditions in a single study. Hence, we first wished to establish the repair efficiencies of these two systems using immunoblot assays in which *Arabidopsis* cells were irradiated with UV and incubated in either the dark or under a black light. Repair kinetics were followed by immunoslot blot analysis of genomic DNA with antibodies that specifically recognize CPDs or (6-4)PPs.

As is apparent in Fig. 1*A*, both UV photoproducts were removed from the genome at a moderate rate when cells were incubated in the dark, such that nearly 60% of (6-4)PPs and CPDs were removed within 4 and 24 h, respectively. However, in the presence of blue light and with cells on ice to prevent excision repair, the repair of both (6-4)PPs and CPDs was significantly faster (Fig. 1*B*), which shows that these cells have a high capacity for the photoenzymatic repair of these photoproducts by specific photolyases (15, 16).

Nonetheless, these results demonstrate that plant cells possess the ability to remove UV photoproducts from their genomes in a light/photolyase-independent manner.

Isolation of Dual-Incision Repair Products. We next wished to determine whether the photolyase-independent (dark) mode of UV photoproduct removal involves a classic dual-incision mechanism that is characteristic of the nucleotide excision repair systems in bacteria, humans, and other organisms (17–19). However, there is currently no in vitro excision repair assay for plant nucleotide excision repair. We therefore adapted the in vivo excision assay that we recently developed in our laboratory for studying nucleotide excision repair in mammalian cells in vivo (12–14). In this assay, cells are lysed at various time points following UV irradiation and the excised oligonucleotide products of nucleotide excision repair are isolated by immunoprecipitation with antibodies against either the repair factor TFIIH (because the excised oligonucleotide is released in a complex with the core repair factor TFIIH) or against specific UV photoproducts (12, 20). The isolated oligonucleotides are then 3′-labeled with either a radiolabeled or biotinylated

Significance

UV wavelengths of sunlight cause damage to genomic DNA in all organisms, including plants. Although UV photoproducts are known to be removed from DNA through the process of nucleotide excision repair in a wide variety of organisms, ranging from bacteria to humans, the mechanism of this repair process in plants has never been examined. Here, using a highly sensitive DNA repair assay that we developed to monitor UV photoproduct repair in vivo, we found that plants remove UV photoproducts from their genomic DNA through a dual-incision mechanism that is nearly identical to that of humans and other eukaryotes.

Author contributions: C.P.S., M.G.K., J.H., L.A.L.-B., and A.S. designed research; F.C., M.K., C.P.S., G.K.-E., J.H., and W.L. performed research; C.P.S., G.K.-E., J.H., and W.L. contributed new reagents/analytic tools; F.C., M.K., C.P.S., M.G.K., G.K.-E., J.H., W.L., L.A.L.-B., and A.S. analyzed data; and C.P.S., M.G.K., and A.S. wrote the paper.

Reviewers: S.L., Lousiana State University; C.L., University of California, Los Angeles; and Y.-J.X., Wright State University.

The authors declare no conflict of interest.

[1]F.C., M.K., and C.P.S. contributed equally to this work.

[2]To whom correspondence should be addressed. Email: aziz_sancar@med.unc.edu.

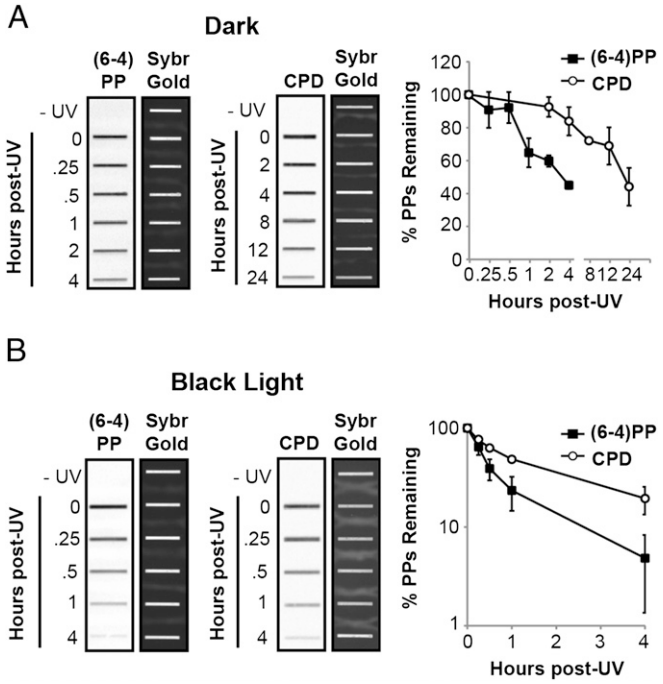

Fig. 1. Immunoslot blot analysis of CPD and (6-4)PP removal from genomic DNA in *Arabidopsis*. (*A*) *Arabidopsis* cells were irradiated with UV (50 J/m^2) and then incubated in the dark at room temperature. The DNA was immobilized on nitrocellulose and probed with antibodies against the indicated UV photoproduct. The graph shows the percentage of CPDs and (6-4)PPs that remained in the genomic DNA at the indicated time points. Each point represents the average (and SD) level of repair from three independent experiments. (*B*) Immunoslot blot analysis of UV photoproduct repair was performed as in *A*, except that cells were incubated on ice and exposed to a black light for the indicated time periods after UV treatment and before isolation of genomic DNA.

nucleotide and the size of the excised fragments are determined on a sequencing gel.

To adapt this general methodology to plant cells, we irradiated an *Arabidopsis* cell line grown in suspension with 50 J/m^2 of 254-nm UV and then lysed the cells at several time intervals after irradiation. Low molecular weight damage-containing DNAs were isolated by immununoprecipitation with UV photoproduct-specific antibodies, 3′-end–labeled with ^{32}P-cordycepin and terminal transferase, separated on sequencing gels, and visualized with a phosphorimager. As shown in Fig. 2*A*, DNA oligonucleotides 11–29 nt in length were clearly observed following the exposure of the plant cells to UV radiation and were not present in nonirradiated cells. Moreover, two distinct populations of DNA oligonucleotides were visible, particularly in the case of the (6-4)PP-containing DNA fragments. These two populations included one with a peak in the range of 23–29 nt in length and a second, smaller series of fragments in the range of 11–22 nt in length. Quantitative analyses of the size distributions of (6-4)PP-containing DNA fragments at various time points following irradiation demonstrated that the DNA oligonucleotides initially showed a mean peak length of 26 nt at early time points and a peak length of 16–18 nt at later time points (Fig. 2*B*). Interestingly, this pattern has been reported previously for human nucleotide excision repair using both in vitro (20–23) and in vivo (12–14, 24, 25) approaches for monitoring repair, which indicates that these UV-induced DNA fragments are bone fide products of nucleotide excision repair in plant cells.

In human nucleotide excision repair, the excised oligonucleotides are initially released from duplex DNA in a tight complex with the repair factor TFIIH (20) and are subsequently released from TFIIH to be degraded or bind to the single-stranded DNA binding protein RPA in a partially degraded state (12, 20, 24). With prolonged incubations, all excision products are degraded to a size that is too small to be detected by this assay. Nucleases present in cells or cell lysates are likely responsible for the degradation of excised oligonucleotides following release from duplex DNA. Indeed, in a fully reconstituted excision repair reaction with the six core excision repair factors TFIIH, RPA, XPA, XPC, XPG, and XPF-ERCC1, there is no degradation of the excision products (20). Nonetheless, the similarity of excision patterns in plants and

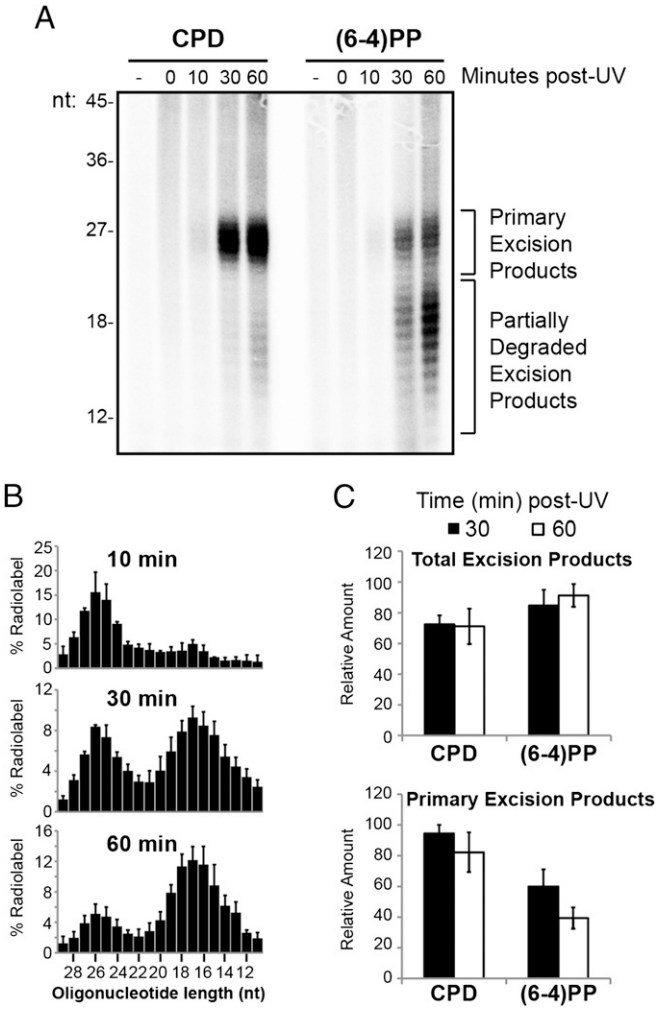

Fig. 2. The dual-incision product in *Arabidopsis*. (*A*) *Arabidopsis* cells were exposed to 50 J/m^2 of UV radiation and then incubated for the indicated periods of time. Cells were then harvested and lysed for extraction of small DNA oligonucleotides. The excised oligonucleotide products of nucleotide excision repair were isolated by immunoprecipitation with antibodies against the indicated UV photoproducts. Oligonucleotides were 3′-end-labeled with ^{32}P-cordycepin and terminal transferase before separation on a sequencing gel and phosphorimager analysis. DNA oligonucleotide standards of the indicated lengths were electrophoresed on all gels. (*B*) Size distribution of (6-4)PP-containing excision products as a function of time following UV irradiation. The phosphorimager signals for oligonucleotides of the indicated lengths in *A* were quantified and normalized against the total radiolabel signal for oligonucleotides 11–29 nt in length. Graphs show the average (and SEM) from two to three independent experiments. (*C*) Excision activity toward CPDs and (6-4)PPs was quantified at the indicated time points from experiments performed as in *A*. Total excision products 11–29 nt in length (*Upper*) or the primary excision products 23–29 nt in length (*Lower*) were quantified and normalized to the maximum signal in each experiment. The data show the average (and SEM) excision activity for each time point from two to three independent experiments.

humans suggests that a similar mechanism of excision and post-excision nucleolytic processing of excised oligonucleotides takes place in plants. Thus, we will refer to the larger species of excised oligonucleotides 23–29 nt in length as the primary or full-length excision products and the smaller species as the partially degraded excision products.

CPDs are generally removed from the human genome at a slower rate than (6-4)PPs because of differences in the ease of recognition by the nucleotide excision repair system. However, with the excision assay we observed relatively robust CPD repair even at early time points following irradiation of plant cells (Fig. 2*A*). Quantitative analyses of total excision products in the range of 11–29 nt from several independent experiments indicated that CPD-containing excision products were nearly as prevalent as oligomers containing (6-4)PPs (Fig. 2*C*, *Upper*). When we restricted our quantitative analysis to just the primary excision products, CPD-containing oligomers were observed at about twice the level of (6-4)PP-containing products following UV irradiation (Fig. 2*C*, *Lower*).

This result appears to conflict with findings from the immunoslot blot assay (Fig. 1*A*) and with results from other organisms studied to date. However, CPDs are formed at an approximate 3:1 ratio relative to (6-4)PPs following UV, and thus the relative abundance of different photoproducts that are formed in DNA following UV exposure should be considered when interpreting photoproduct removal rates using different assays of repair. Nonetheless, these results point to a potential shortcoming of the in vivo excision assay as a quantitative tool arising because excision products are simultaneously formed and degraded. In this particular case, in plant cells, the CPD photoproducts are removed from the genome more slowly than (6-4)PPs, and the CPD-containing excised oligonucleotides appear to be degraded much more slowly. The degradation rates in *Arabidopsis* may be influenced by the presence of photolyases, which are known to bind to photoproducts in both single- and double-stranded DNA. Of note, the photolyases may also influence the rate of excision repair. It has been shown in *Escherichia coli* that the binding of photolyase to CPDs accelerates the rate of the UvrABC excision nuclease by a factor of 2–3 because binding of photolyase to CPDs in the dark generates a relatively stable protein–DNA complex with higher affinity to the $UvrA_2B_1$ damage recognition subcomplex of the excision nuclease (26).

Determination of 5′ and 3′ Incision Sites. We next wished to map the locations of the incision sites relative to the photoproducts to compare the dual-incision patterns between humans and plants. Primary (6-4)PP- and CPD-containing excised oligonucleotides of ∼24–29 nt in length were therefore isolated by immunoprecipitation with the appropriate damage-specific antibody and gel extraction before treatment with either T4 DNA polymerase or RecJ nuclease, which possess 3′→5′ and 5′→3′ exonuclease activities, respectively. The UV photoproducts are barriers to the nucleolytic activities of these enzymes (12, 21, 27, 28), which therefore allowed us to determine the distances between the UV-adducted nucleotides and the 5′ and 3′ ends of the excised oligonucleotides (Fig. 3*A*).

To determine the 5′ incision site, the isolated primary oligonucleotides containing (6-4)PPs or CPDs were 5′ labeled with polynucleotide kinase and then digested in the 3′ to 5′ direction with T4 DNA polymerase/exonuclease. As shown in Fig. 3*B*, this treatment produced fragments 20–23 nt in length, which indicates that the 5′ incision occurs 18–21 nt 5′ to the photoproduct in *Arabidopsis*. We note that these incision sites are similar for both excised (6-4)PP and CPD oligonucleotides and are within the range of incisions observed in humans (21), mice (29), hamster (29), frogs (23), and yeast (30).

To determine the 3′ incision site relative to the photoproducts, excised oligonucleotides containing either CPDs or (6-4)PPs were isolated by immunoprecipitation, radiolabeled at the 3′ end with terminal transferase, and then treated with Rec J exonuclease, which degrades single-stranded DNA in the 5′ to 3′ direction. The

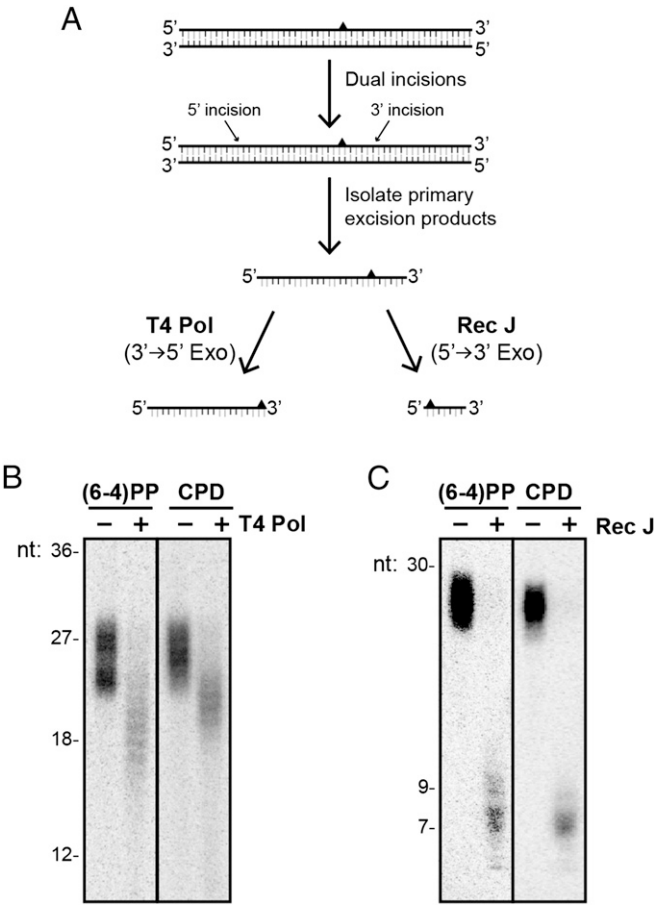

Fig. 3. Locations of the 5′ and 3′ incision sites in *Arabidopsis* nucleotide excision repair. (*A*) Schematic of methodology for determining the locations of the 5′ and 3′ incision sites relative to the UV photoproducts. CPD- and (6-4)PP-containing excision products were isolated from UV-irradiated *Arabidopsis* cells by immunoprecipitation and then either 5′- or 3′-radiolabeled. Primary excision products 24–29 nt in length were extracted from a sequencing gel, purified, and then treated with either T4 DNA polymerase (T4 Pol) or RecJ nuclease, which digest DNA in the 3′→5′ and 5′→3′ directions, respectively. DNAs were then separated on a sequencing gel. (*B*) Determination of the 5′ incision site by treatment of primary excised oligonucleotides with T4 DNA polymerase. (*C*) Mapping of the 3′ incision site by treatment of the primary excision products with RecJ nuclease. DNA oligonucleotide standards of known length were electrophoresed on all gels to determine the size of the digested DNA fragments.

products were then analyzed on a sequencing gel. As shown in Fig. 3*C*, treatment of excised fragments 24–29 nt in length with RecJ gave rise to fragments of 6–8 nt, which indicates that the 3′ incision site is 4–6 nt from the photoproduct. Importantly, digestion of both excised CPD- and (6-4)PP-containing oligonucleotides with RecJ gave rise to oligomers of essentially the same size, which indicates the same 3′ incision pattern of both photoproducts.

Dual Incisions in Eukaryotes. Dual incisions at sites bracketing UV photoproducts have been detected in bacteria (31), the archaeon *Methanobacterium thermoautotrophicum* (32), humans (21), yeast (30), hamster (29), mice (29), frogs (23), and now in *Arabidopsis*. Based on these findings, the following generalizations can be made. In bacteria and other prokaryotes, dual incisions occur 7 nt 5′ and 3 nt 3′ to the damage to result in removal of UV-induced photoproducts in the form of oligonucleotides 12–13 nt in length (Fig. 4). In mammals, vertebrates, yeast, and plants, the 5′ incision is ∼20 nt 5′ and ∼5 nt 3′ to the damage, which releases the UV photoproducts

in fragments with a median size of 26–27 nt. Whether these dual-incision patterns are universal to all prokaryotic and eukaryotic organisms remains to be seen.

Discussion

Although nucleotide excision repair appears to be universal in cellular organisms ranging from mycoplasma to humans (17–19, 32), it has only been studied in a select group of model organisms. It is essential that this repair system is analyzed biochemically in more species for a comprehensive understanding of its molecular mechanisms and its evolutionary changes across species. Our general methodology for visualizing excision repair in vivo in human and plant cells should therefore facilitate the characterization of nucleotide excision repair mechanisms in additional species across the three domains of life.

Using the in vivo excision assay, we found that the basic molecular mechanism of excision repair in a plant species is essentially the same as the human dual-incision mechanism. Analyses of the *Arabidopsis* and rice genomes reveal that they contain homologs of all of the human excision repair proteins, with the exception of the damage recognition protein XPA (xeroderma pigmentosum, complementation group A) (33). This is a critical component in human nucleotide excision repair, and in its absence there is no detectable excision repair either in vivo or in vitro. Therefore, its apparent absence in plants is rather surprising. However, we note that XPA is an intrinsically unstructured protein (34) and its primary structure is not highly conserved across species. It is conceivable that an XPA ortholog not detectable by standard filtering programs participates in plant excision repair or that a protein unrelated to XPA, but nevertheless possessing similar properties, substitutes for XPA to aid in recruiting and targeting key excision repair factors TFIIH and XPF during excision repair. The use of the in vivo biochemical excision assay in conjunction with genetic strategies could therefore aid in identifying a plant XPA ortholog as well as other genes that serve regulatory roles in excision repair.

Finally, we expect that the in vivo excision assay can be used to readily determine the mechanism of nucleotide excision repair in other organisms, including in the archaea. Although some archaeal species have acquired genes with similarity to the *E. coli* uvrABC system, likely through horizontal gene transfer, most archaea appear to possess genes with greater homology to a subset of the eukaryotic-type repair factors (35, 36). Thus, the application of the in vivo excision assay to previously unstudied organisms should facilitate the identification of novel excision repair factors and possibly the characterization of unique excision repair mechanisms throughout the evolutionary tree of life.

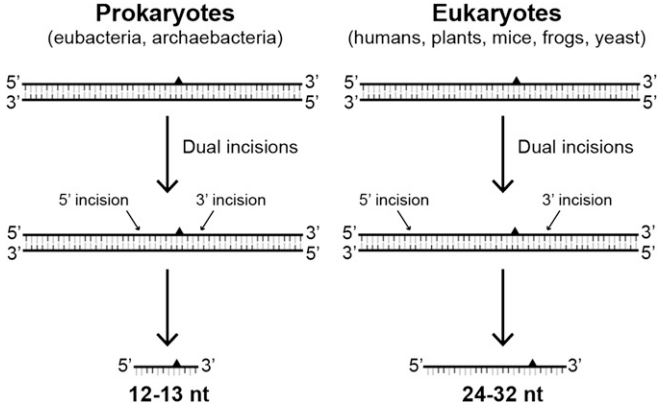

Fig. 4. Models of nucleotide excision repair in prokaryotes and eukaryotes. In prokaryotic organisms that possess genes with homology to the bacterial *uvrABC* genes, such as *E. coli* and the archaeal organism *M. thermoautotrophicum*, dual incisions occur ~7 nt 5′ and 3 nt 3′ to the UV photoproduct. These dual incisions therefore result in the generation of 12- to 13-nt-long damage-containing oligonucleotides. Note that the mechanism of excision repair in most archaeal species, which lack the uvrABC system but possess genes with similarity to many of the eukaryotic repair factors, is unknown. In humans, plants, and other eukaryotic species, dual incisions take place ~20 nt 5′ and 5 nt 3′ to the lesion, which removes the damage from the genome in the form of oligonucleotides 24–32 nt in length.

Materials and Methods

***Arabidopsis thaliana* Cell Culture.** The *A. thaliana* ecotype Columbia cell line T87 was obtained from the *Arabidopsis* Biological Resource Center at The Ohio State University. Cells were maintained as suspensions in NT-1 medium (4.3 g MS salt, 30 g sucrose, 0.18 g KH_2PO_4, 100 μL of 10 mg/mL Thiamine stock, 220 μL of 2 mg/mL 2,4-D stock, and 100 mg myo-inositol per L, with the pH adjusted to 5.8 with 5 M NaOH) under continuous light at 24 °C and shaken at 120 rpm on a Barnstead MAX Q2000 Open-Air Platform Shaker. Every 7 d, cells were subcultured into fresh NT-1 media [1:20 (vol/vol)] in 500-mL Erlenmeyer flasks.

UV Irradiation and Lysate Preparation. All steps were performed in a dark room with dim yellow light illumination. UV irradiation was performed as described previously (37). Briefly, 10 mL of chilled cells in 100-mm tissue-culture dishes were placed on ice-water under a GE germicidal lamp that emits primarily 254-nm UV light (UV-C). Cells were exposed to 50 J/m^2 of UV-C. Following irradiation, dishes were incubated by floatation on room temperature water for the indicated lengths of time. For photoreactivation, cells on ice were exposed to a black light that emits primarily 365-nm light for the indicated times. Following repair, the cells (typically 4.5 g, wet weight) were collected by centrifugation and were placed in dry ice. Frozen cells under liquid nitrogen were ground using a mortar and pestle, and powder was stored at −80 °C. The powders were then resuspended in 100 μL of STES buffer (200 mM Tris·HCl pH 8.0, 500 mM NaCl, 0.1% SDS, 10 mM EDTA). Then, 100 μL of phenol:chloroform (20:1) and 200 μL of acid washed glass beads (425–500 nm in diameter) were added to each tube. Tubes were vortexed for 15 min at 4 °C, and then the cell lysates were centrifuged at maximum speed for 10 min at 4 °C in a microcentrifuge. Supernatants consisting of the liquid above the glass beads and containing the cell lysates were collected for further processing.

Immunoslot Blot Analysis. Cell lysates were extracted with phenol–chloroform–isoamyl alcohol and then genomic DNA was collected by ethanol precipitation. RNA-free genomic DNA was isolated using a QIAquick PCR purification kit (Qiagen) with RNase A treatment. The quality and quantity of genomic DNA were assessed by using a Nano Drop 1000 spectrophotometer.

Repair of CPDs and (6-4)PPs was measured as previously described (37). Briefly, genomic DNA [100 ng for CPD detection, and 250 ng for (6-4)PP dectection] was denatured by heating at 94 °C for 10 min. Samples were then chilled in ice water, and cold ammonium acetate (2 M) was added to a final concentration of 1 M. Samples (in duplicate) were immobilized on nitrocellulose membranes using a Bio-Dot SF apparatus (Bio-Rad). Membranes were baked for 1.3 h at 80 °C in a preheated vacuum oven and then blocked in PBS containing 5% (wt/vol) nonfat dry milk and 0.1% Tween 20 for 1 h at room temperature with gentle shaking. Immunodetection of CPDs and (6-4)PPs was carried out by incubation for 16 h at 4 °C with anti-CPD (Cosmo Bio; 1:8,000 dilution) or anti-(6-4)PP (Cosmo Bio; 1:4,000 dilution) antibodies in PBS containing 0.1% Tween 20. Anti-mouse secondary antibody (NA931V, GE Healthcare) conjugated with horseradish peroxidase was then incubated with the membrane, and the photoproduct signals were detected using ECL Primer reagent (GE Healthcare) and a Bio-Rad Chemi-Doc imager. Membranes were then stained with Sybr Gold to detect total DNA. Quantification was performed with ImageQuant 5.2 software, and the repair data (average and SD) from three independent experiments were plotted.

In Vivo Excision Repair Assay. The method for the isolation and detection of the excised oligonucleotide products of nucleotide excision repair was adapted from previous studies in human cells (12–14, 24, 25). *Arabidopsis* cell lysates were incubated with RNase A (1:500; R4642 Sigma) for 10 min at room temperature and then deproteinized by the addition of SDS to a final concentration of 0.33% (from a 10% stock) and incubation with Proteinase K (1:400; P8107S New England Biolabs) for 30 min at 55 °C. Following phenol chloroform extraction and ethanol precipitation, DNA samples were resuspended in 10 μL of water. Immunoprecipitations were performed as described previously (12) to isolate excised oligonucleotides containing CPDs or (6-4)PPs. Briefly, for each reaction, 5 μL of protein G Dynabeads (Invitrogen, catalog no. 10003D) slurry and 5 μL of anti-rabbit Dynabeads (Invitrogen, catalog no. 11203D) slurry were washed three times with 50 μL of wash buffer I (20 mM Tris·HCl pH 8.0, 2 mM EDTA, 150 mM NaCl, 1% Triton X-100, and 0.1% SDS) and then

incubated with 1 μL of rabbit anti-mouse IgG and 1 μL of anti-CPD or anti-(6-4)PP antibody in 20 μL of immunoprecipitation buffer (20 mM Tris·HCl pH 8.0, 2 mM EDTA, 150 mM NaCl, 1% Triton X-100, and 0.5% sodium deoxycholate) for 3 h at 4 °C. After incubation, beads were separated from the liquid using a magnet and then mixed with 100 μL of immunoprecipitation buffer and 10 μL of DNA. The mixtures were rotated at 4 °C overnight. The beads were then washed sequentially with 200 μL each of wash buffer I, wash buffer II (20 mM Tris·HCl pH 8.0, 2 mM EDTA, 500 mM NaCl, 1% Triton X-100, and 0.1% SDS), wash buffer III (10 mM Tris·HCl pH 8.0, 1 mM EDTA, 150 mM LiCl, 1% Nonidet P-40, and 1% sodium deoxycholate), wash buffer IV (100 mM Tris·HCl pH 8.0, 1 mM EDTA, 500 mM LiCl, 1% Nonidet P-40, and 1% sodium deoxycholate), and finally twice with TE (10 mM Tris·HCl pH 8.0 and 1 mM EDTA). The oligonucleotides containing UV photoproducts were eluted by incubation with 100 μL of elution buffer (50 mM $NaHCO_3$, 1% SDS, and 20 μg/mL glycogen) at 65 °C for 15 min. The eluted DNA was then isolated by phenol/ chloroform extraction and followed by ethanol precipitation. For 3′-end labeling, the immunoprecipitated DNA was incubated with 20 units of terminal deoxynucleotidyl transferase (New England Biolabs) and 1 μCi of [α-^{32}P]-3′-deoxyadenosine 5′-triphosphate (cordycepin 5′-triphosphate; Perkin-Elmer Life Sciences) for 1 h at 37 °C in a 50-μL reaction according to the manufacturer's protocol (New England Biolabs). For 5′-end labeling, the immunopurified DNA was treated with 1 unit of FastAP thermosensitive alkaline phosphatase (Thermo) in 45 μL of 1× T4 polynucleotide kinase buffer (New England Biolabs) for 20 min at 37 °C. After heat inactivation (75 °C, 5 min), the reaction was incubated with 10 units of T4 polynucleotide kinase (New England Biolabs) and 3 μCi of [γ-^{32}P]-ATP (MP Biomedicals) for 1 h at 37 °C. The labeling reaction was heat-inactivated (65 °C for 20 min) and then incubated with 1 μL of RNase A/T1 mixture (Thermo) for 30 min at 37 °C to remove contaminating RNA. After phenol-chloroform extraction and ethanol precipitation, radiolabeled DNAs were resuspended in formamide dye-loading solution, heat-denatured, and then resolved in 11% (wt/vol) denaturing sequencing gels and visualized using a Typhoon TRIO+ phosphorimager (GE Healthcare). Excision repair activity was quantified using ImageQuant software (v5.2, GE Healthcare).

Identification of Incision Sites. For 5′→3′ digestion, gel-purified, 3′-end-labeled DNA was incubated with 22.5 units of $RecJ_f$ (New England Biolabs) for 1 h at 37 °C in a 5-μL reaction according to the recommendations of the manufacturer. Products were then ethanol-precipitated and resolved on an 11% sequencing gel. For 3′→5′ digestion, 5′-end-labeled, gel-purified DNA was incubated with 0.6 units of T4 DNA polymerase (New England Biolabs) for 1 h at 37 °C in a 4-μL reaction according to the manufacturer's recommendations. Reactions were stopped by adding 10 μL of formamide loading buffer and heating for 5 min at 95 °C. Samples were separated on 11% denaturing sequencing gels.

ACKNOWLEDGMENTS. This work was supported by National Institutes of Health Grant R01GM32833 (to A.S.); the Scientific and Technological Research Council of Turkey (TÜBİTAK) (G.K.-E.); and the Hacettepe University Scientific Research Projects Coordination Unit (G.K.-E.).

1. Bleuyard JY, Gallego ME, White CI (2006) Recent advances in understanding of the DNA double-strand break repair machinery of plants. *DNA Repair (Amst)* 5(1):1–12.
2. Bray CM, West CE (2005) DNA repair mechanisms in plants: Crucial sensors and effectors for the maintenance of genome integrity. *New Phytol* 168(3):511–528.
3. Britt AB (1999) Molecular genetics of DNA repair in higher plants. *Trends Plant Sci* 4(1):20–25.
4. Kimura S, Sakaguchi K (2006) DNA repair in plants. *Chem Rev* 106(2):753–766.
5. Vonarx EJ, Mitchell HL, Karthikeyan R, Chatterjee I, Kunz BA (1998) DNA repair in higher plants. *Mutat Res* 400(1-2):187–200.
6. Britt AB (1995) Repair of DNA damage induced by ultraviolet radiation. *Plant Physiol* 108(3):891–896.
7. Nakajima S, et al. (1998) Cloning and characterization of a gene (UVR3) required for photorepair of 6-4 photoproducts in *Arabidopsis thaliana*. *Nucleic Acids Res* 26(2): 638–644.
8. Li J, Uchida T, Todo T, Kitagawa T (2006) Similarities and differences between cyclobutane pyrimidine dimer photolyase and (6-4) photolyase as revealed by resonance Raman spectroscopy: Electron transfer from the FAD cofactor to ultraviolet-damaged DNA. *J Biol Chem* 281(35):25551–25559.
9. Li J, et al. (2010) Dynamics and mechanism of repair of ultraviolet-induced (6-4) photoproduct by photolyase. *Nature* 466(7308):887–890.
10. Howland GP (1975) Dark-repair of ultraviolet-induced pyrimidine dimers in the DNA of wild carrot protoplasts. *Nature* 254(5496):160–161.
11. Quaite FE, Takayanagi S, Ruffini J, Sutherland JC, Sutherland BM (1994) DNA damage levels determine cyclobutyl pyrimidine dimer repair mechanisms in alfalfa seedlings. *Plant Cell* 6(11):1635–1641.
12. Hu J, et al. (2013) Nucleotide excision repair in human cells: Fate of the excised oligonucleotide carrying DNA damage in vivo. *J Biol Chem* 288(29):20918–20926.
13. Choi JH, et al. (2014) Highly specific and sensitive method for measuring nucleotide excision repair kinetics of ultraviolet photoproducts in human cells. *Nucleic Acids Res* 42(4):e29.
14. Choi JH, Kim SY, Kim SK, Kemp MG, Sancar A (2015) An integrated approach for analysis of the DNA damage response in mammalian cells: Nucleotide excision repair, DNA damage checkpoint, and apoptosis. *J Biol Chem* 290(48):28812–28821.
15. Sancar A (2003) Structure and function of DNA photolyase and cryptochrome blue-light photoreceptors. *Chem Rev* 103(6):2203–2237.
16. Sancar A (2004) Photolyase and cryptochrome blue-light photoreceptors. *Adv Protein Chem* 69:73–100.
17. Reardon JT, Sancar A (2005) Nucleotide excision repair. *Prog Nucleic Acid Res Mol Biol* 79:183–235.
18. Sancar A (1996) DNA excision repair. *Annu Rev Biochem* 65:43–81.
19. Wood RD (1997) Nucleotide excision repair in mammalian cells. *J Biol Chem* 272(38): 23465–23468.
20. Kemp MG, Reardon JT, Lindsey-Boltz LA, Sancar A (2012) Mechanism of release and fate of excised oligonucleotides during nucleotide excision repair. *J Biol Chem* 287(27):22889–22899.
21. Huang JC, Svoboda DL, Reardon JT, Sancar A (1992) Human nucleotide excision nuclease removes thymine dimers from DNA by incising the 22nd phosphodiester bond 5′ and the 6th phosphodiester bond 3′ to the photodimer. *Proc Natl Acad Sci USA* 89(8):3664–3668.
22. Huang JC, Sancar A (1994) Determination of minimum substrate size for human excinuclease. *J Biol Chem* 269(29):19034–19040.
23. Svoboda DL, Taylor JS, Hearst JE, Sancar A (1993) DNA repair by eukaryotic nucleotide excision nuclease. Removal of thymine dimer and psoralen monoadduct by HeLa cell-free extract and of thymine dimer by *Xenopus laevis* oocytes. *J Biol Chem* 268(3): 1931–1936.
24. Kemp MG, Gaddameedhi S, Choi JH, Hu J, Sancar A (2014) DNA repair synthesis and ligation affect the processing of excised oligonucleotides generated by human nucleotide excision repair. *J Biol Chem* 289(38):26574–26583.
25. Hu J, Adar S, Selby CP, Lieb JD, Sancar A (2015) Genome-wide analysis of human global and transcription-coupled excision repair of UV damage at single-nucleotide resolution. *Genes Dev* 29(9):948–960.
26. Sancar A, Franklin KA, Sancar GB (1984) *Escherichia coli* DNA photolyase stimulates uvrABC excision nuclease in vitro. *Proc Natl Acad Sci USA* 81(23):7397–7401.
27. Burdett V, Baitinger C, Viswanathan M, Lovett ST, Modrich P (2001) In vivo requirement for RecJ, ExoVII, ExoI, and ExoX in methyl-directed mismatch repair. *Proc Natl Acad Sci USA* 98(12):6765–6770.
28. Doetsch PW, Chan GL, Haseltine WA (1985) T4 DNA polymerase (3′-5′) exonuclease, an enzyme for the detection and quantitation of stable DNA lesions: The ultraviolet light example. *Nucleic Acids Res* 13(9):3285–3304.
29. Reardon JT, Thompson LH, Sancar A (1997) Rodent UV-sensitive mutant cell lines in complementation groups 6-10 have normal general excision repair activity. *Nucleic Acids Res* 25(5):1015–1021.
30. Guzder SN, Habraken Y, Sung P, Prakash L, Prakash S (1995) Reconstitution of yeast nucleotide excision repair with purified Rad proteins, replication protein A, and transcription factor TFIIH. *J Biol Chem* 270(22):12973–12976.
31. Sancar A, Rupp WD (1983) A novel repair enzyme: UVRABC excision nuclease of *Escherichia coli* cuts a DNA strand on both sides of the damaged region. *Cell* 33(1): 249–260.
32. Ogrünç M, Becker DF, Ragsdale SW, Sancar A (1998) Nucleotide excision repair in the third kingdom. *J Bacteriol* 180(21):5796–5798.
33. Kunz BA, Anderson HJ, Osmond MJ, Vonarx EJ (2005) Components of nucleotide excision repair and DNA damage tolerance in *Arabidopsis thaliana*. *Environ Mol Mutagen* 45(2-3):115–127.
34. Iakoucheva LM, et al. (2001) Identification of intrinsic order and disorder in the DNA repair protein XPA. *Protein Sci* 10(3):560–571.
35. Rouillon C, White MF (2011) The evolution and mechanisms of nucleotide excision repair proteins. *Res Microbiol* 162(1):19–26.
36. Grogan DW (2015) Understanding DNA repair in hyperthermophilic archaea: Persistent gaps and other reasons to focus on the fork. *Archaea* 2015:942605.
37. Gaddameedhi S, et al. (2010) Similar nucleotide excision repair capacity in melanocytes and melanoma cells. *Cancer Res* 70(12):4922–4930.